Anomalous Conductance Distribution in Quasi-One Dimension: Possible Violation of One-Parameter Scaling Hypothesis

Pritiraj Mohanty[1] and Richard A. Webb[2]

[1] *Department of Physics, Boston University, 590 Commonwealth Avenue, Boston, MA 02215*

[2] *Department of Physics, Center for Superconductivity Research, University of Maryland, College Park, MD 20742*

arXiv:cond-mat/0204298v1 [cond-mat.mes-hall] 13 Apr 2002

We report measurements of conductance distribution in a set of quasi-one-dimensional gold wires. The distribution includes the second cumulant or the variance which describes the universal conductance fluctuations, and the third cumulant which denotes the leading deviation. We have observed an asymmetric contribution—or, a nonvanishing third cumulant—contrary to the expectation for quasi-one-dimensional systems in the noninteracting theories in the one-parameter scaling framework, which include the perturbative diagrammatic calculations and the random matrix theory.

Scaling theory of Anderson localization is the starting point of mesoscopic physics [1]. It forms the basis of our understanding of low-dimensional metals as well as various conductor-insulator transitions. The theory is based on the one-parameter scaling hypothesis which argues that the conductance G is the only relevant parameter that controls its variation with size L, implying

$$\frac{\partial \ln g}{\partial \ln L} = \beta(g); \qquad g \equiv \frac{G}{e^2/h}, \tag{1}$$

where $\beta(g)$ is a universal function of the dimensionless conductance g alone. The perturbative calculations [2] in terms of $1/g$ find the following Gell-Mann-Low $\beta(g)$-function for small deviations from the ohmic behavior in good metals ($g \gg 1$):

$$\beta(g) = (d-2) + \alpha/g + \cdots \tag{2}$$

The first term represents the Ohm's law, and the second one is the leading quantum correction—for example, from weak localization ($\alpha \simeq -1$). The scaling hypothesis has been confirmed by field-theoretical calculations in the nonlinear σ-model [3].

One-parameter scaling must be understood in terms of the entire conductance distribution; this was realized almost immediately after its discovery [4]. Another reason for studying conductance distribution for the interpretation of one-parameter scaling pertains to the sample-specific conductance fluctuations [5,6] with variance $\langle \delta g^2 \rangle \sim 1$, the discovery of which raised the problem of how to sum up a diverging series of quantum corrections of order one ($\delta G \sim e^2/h$) in low dimensions $d \leq 2$. However, the validity of the perturbation theory (in $1/g$) was established, contingent upon one-parameter scaling [7]. Large conductance fluctuations were found to cause an instability of the one-parameter scaling near the localization transition for $g \leq 1$, leading to fluctuations which deviate from gaussian to one with a log-normal tail. However, in the metallic region ($g \gg 1$), for small fluctuations the distribution was found to be gaussian [7]. These fluctuations are essentially the universal conductance fluctuations (UCF), independent of sample parameters such as mean free path l_e and average conductance $\langle g \rangle$ (not including the effects of temperature and dephasing). Further support for one-parameter scaling in presence of conductance fluctuations was obtained by calculations in random matrix theory [8,9]. In general, in the metallic regime,

$$\langle g^n \rangle \propto \langle g \rangle^{2-n}, \quad n < g_0. \tag{3}$$

g_0 is the mean conductance at the scale l_e. For $n = 2$, one obtains the UCF, independent of $\langle g \rangle$. Higher cumulants for $n > 2$ are small, and the distribution is dominantly gaussian. For $n > g_0$, the magnitudes of higher order cumulants increase rapidly as $\langle g^n \rangle \propto e^{n^2/g_0}$; this leads to the log-normal distribution [10] in the non-metallic region near localization ($g \leq 1$).

Any deviation from the normal (gaussian) distribution can be divided into two characteristic parts: deviation in the vicinity of the maximum, and the asymptotics near the tail. The tail is governed by high order cumulants, whereas the center of the distribution is determined by the lowest non-trivial cumulants—i.e., the third and the fourth cumulants (n=3 and 4). Recent calculations in random matrix theory [11], based on a local maximum-entropy approach in the Landauer picture, found that for a unitary ensemble ($B \neq 0$) the third cumulant vanishes in quasi-one dimension [12]. This result was confirmed by calculations in the microscopic diagrammatic theory [13], which further added that the third cumulant or the skewness is negative in quasi-2D and positive in 3D.

In the experiments reported in this Letter, we find that (a) the conductance distribution in quasi-1D metallic ($g \geq 8$) wires is not symmetric, (b) the third cumulant is non-zero and large, and furthermore, (c) it is positive. The experimental artifacts as well as the effects of temperature and dephasing are expected to go in the opposite direction—that is, they work to symmetrize the distribution and reinforce the gaussian. With the increase of temperature from 38 mK to 300 mK, the asymmetry indeed vanishes. The observed skewness at low temperature is

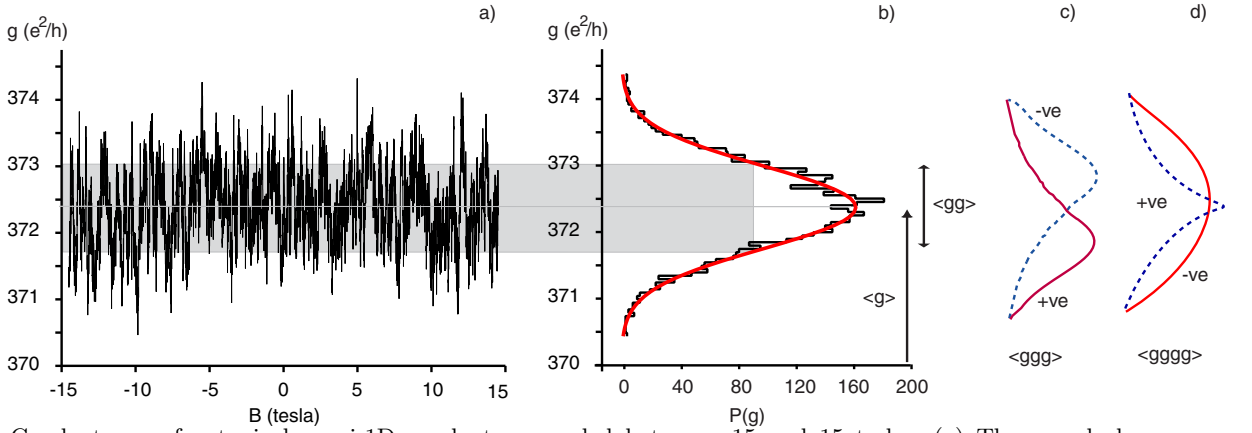

FIG. 1. Conductance of a typical quasi-1D conductor sampled between -15 and 15 tesla. (a) The sample has a mean conductance $\langle g \rangle$ of 372.3. (b) The conductance distribution $P(g)$ constructed from (a). $P(g)$ is gaussian around the mean $\langle g \rangle$, and hence, dominated essentially by universal conductance fluctuations (UCF) or the second cumulant (variance) $\langle gg \rangle$, which determines the full width at half maximum. (c) A distribution whose third cumulant $\langle ggg \rangle$ is substantially different from that of a normal gaussian distribution is schematically shown.(d) The schematic representation shows a distribution whose fourth cumulant $\langle gggg \rangle$ varies greatly from a gaussian.

not reminiscent of a log-normal tail expected at the onset of localization. All this suggests the failure of perturbation theory with renormalized conductance allowed by the scaling procedure, which is equivalent to the summation of all the quantum corrections. As is known, the divergent terms corresponding to the quantum corrections cannot be summed for $d \leq 2$ in a perturbative framework with the un-renormalized classical conductance. In short, a substantial deviation from the gaussian in the metallic region strongly suggests the breakdown of one-parameter scaling procedure, since one needs more than one parameter—the higher order cumulants, to describe the distribution. Its failure in $d < 2$ is serious, as this is where it is supposed to be robust and free from theoretical problems [14]. However, previous experiments on conductance distribution have not addressed this issue [15].

We have measured the full conductance distribution in a set of quasi-1D gold conductors with two high-conductance (high-g) and two low-conductance (low-g) samples, whose dimensions are given in Table I. The dimensionless conductance in the samples is 372, 473, 10.8, and 8.9 at 4 K. The high-g samples, 1d-A and 1d-B, are phase-coherent rings with $L < L_\phi$, the decoherence length. The low-g samples, 1d-C and 1d-D, are long wires; the elastic mean free path l_e is 13.3 nm, and 11.0 nm, and diffusion constant D is 6.06 $\times 10^{-3}$ m^2/s, and 5.02 $\times 10^{-3}$ m^2/s. From the weak localization measurements L_ϕ in 1d-C and 1d-D samples is found to be ~ 4 μm at 38 mK. These samples are designed for two-probe measurements with no other outcoming leads to allow for proper comparison with random matrix theory, valid only for two-probe measurements. We have also measured the conductance distribution in other quasi-1D wires and rings in two-probe and four-probe configurations. Our experimental findings reported here are consistent with the data obtained in these additional samples–that is, the high-g samples and the low-g samples behave differently.

The ensemble for generating the conductance distribution is created by sweeping the magnetic field up to $\pm$ 15 tesla. In the construction and the analysis of the distribution, we have taken following considerations into account: (a) In order to obtain a large number of statistically independent intervals, samples were designed to have large width w and L_ϕ for short correlation scale $B_c \sim \frac{h/e}{wL_\phi}$. However, the requirement of quasi-one dimensionality prevented us from increasing w arbitrarily. The samples studied here represent the optimized set of parameters under the present experimental conditions. (b) Data sets containing instrumental fluctuations were removed. This was achieved by conducting the magnetic field sweep repeatedly, and identifying the large irreproducible fluctuations. Additionally, the positive-field ($B > 0$) and negative-field ($B < 0$) parts of the data were compared for the $g(B) = g(-B)$ symmetry in the case of two-probe samples. In the analysis of the data from the four-probe samples, the asymmetric part, which has its origin in the non-local contributions [16], was removed. (c) To check for the consistency in our analysis, cumulants were also determined from the data binned into sizes larger than the correlation scale $B_c \sim \frac{h/e}{wL_\phi}$. This ensures that the binned data points are statistically uncorrelated even in the sense of UCF–that is, each binned data point represents a conductance fluctuation due to an independent set of interference paths; this procedure reduces the number of points to typically 1000, and hence detriments the statistics by a factor of 2 (for 1d-A and 1d-B) and 3 (for 1d-C and 1d-D). (d) For the calculation of the cumulants, data points between -0.04 to +0.04 tesla, the weak localization corrections, were removed. Thus the data truly represents a unitary ensemble for the purpose of comparison to random matrix theory.

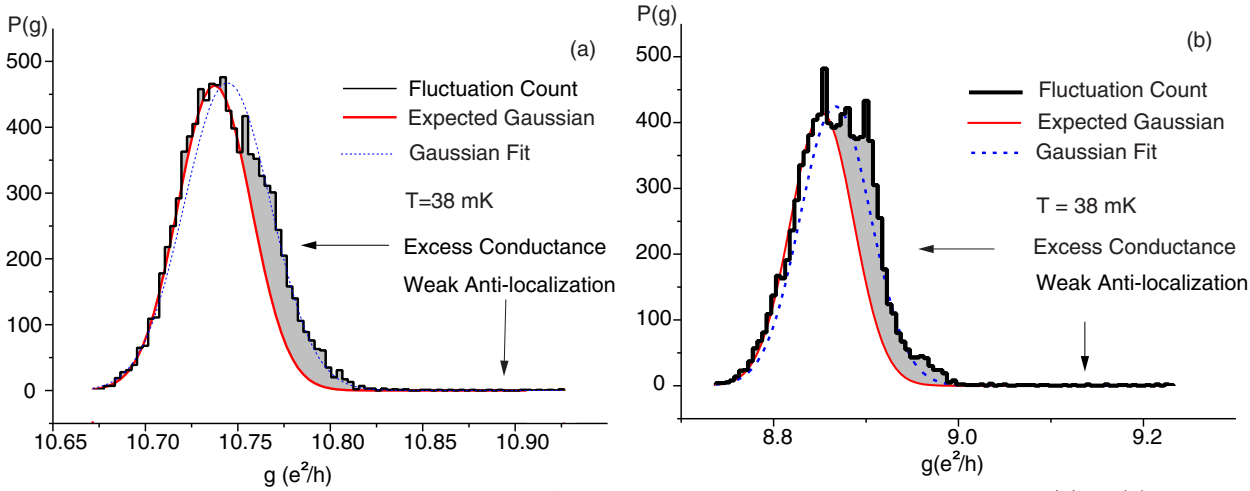

FIG. 2. Conductance of two representative quasi-1D Au wires at 38 mK with a mean conductance $\langle g \rangle$ of (a) 10.75 and (b) 8.85. The histograms are constructed from an ensemble of $\sim$ 9400 samples. The gaussian part of the distribution displays the UCF contribution. The long tail towards higher conductance represents the weak-anti-localization contribution (not included in the evaluation of the cumulants). Unlike in Fig. 1, the distributions are manifestly asymmetric. The shaded areas depict the deviation from the expected gaussian by the higher order contributions ($2 < n \ll g_0$); and the shape indicates a large third cumulant $\langle ggg \rangle$ with a positive coefficient. The dotted curve in both figures is the best gaussian fit to the data.

Fig. 1 displays a typical magnetoconductance trace for the sample 1d-A. We identify the first cumulant—the mean $\langle g \rangle$, and the second cumulant–the variance $\langle gg \rangle$. The UCF contribution $\langle gg \rangle$ is the universal part of the distribution, independent of $\langle g \rangle$ or l_e. This UCF part is a gaussian centered—and symmetric—around $\langle g \rangle$. Fig. 1(c) shows the schematics for distributions whose third cumulant $\langle ggg \rangle$ or the asymmetric deviation from the gaussian is large. The fourth cumulant $\langle gggg \rangle$ or kurtosis, shown schematically in Fig. 1(d), determines the symmetric shape deviation; its positive or negative values represent deviations leading to sharp or flat distributions respectively. As shown in Fig. 1(b), the distribution for the sample 1d-A is a gaussian with undetectable deviations up to the fourth order.

Fig. 2 shows the distributions $P(g)$ for the two low-g samples at 38 mK. In both the samples, 1d-C and 1d-D, a strong deviation from the gaussian is observed with the striking aspect that the asymmetry is present on the high-g side of the mean, and the low-g part of the distribution fits to a gaussian extremely well. The deviation is predominantly in the vicinity of the maximum, and is not reminiscent of a log-normal tail.

Temperature and dephasing tend to reduce the size of the fluctuations and make the distribution gaussian. By raising the temperature to 300 mK, we indeed find that $P(g)$ becomes a gaussian in both the samples, as shown in Fig. 3. This also serves as an important experimental check to ensure that the deviations observed at low temperature are not due to instrumental artifacts. Quantitative estimate of the deviation is difficult, considering the number of statistical independent data points accumulated between -15 and 15 tesla. N = 4800 for 1d-A and 1d-B, and N = 9391 for 1d-C and 1d-D. The variance $\langle gg \rangle$ in the high-g samples ($L < L_\phi$) is consistent with the UCF theory [17], which includes temperature through energy averaging. Data from the low-g samples agree with theory, which includes both temperature ($L_\phi > L_T$, the Thouless length) and dephasing ($L_\phi < L$) effects:

$$\langle gg \rangle_{expt} \simeq \frac{8\pi}{3} \frac{L_\phi L_T^2}{L^3}. \tag{4}$$

The third cumulant, $\langle ggg \rangle$ is within the statistical error bar for the high-g samples 1d-A and 1d-B. However, the low-g samples have a large numerical value of $\langle ggg \rangle$, as would be expected from Fig. 2. The positive value argues that the two samples are not in the quasi-2D regime, where the expected value is both negative and small ($-0.0020\langle g^{-1} \rangle \sim -0.0002$). Beacuse of poor statistics, it is difficult to discern the fourth order deviation $\langle gggg \rangle$ from the data, though it appears to be non-zero and negative.

It is clear that the third cumulant of conductance distribution is non-zero, contrary to the random matrix theory and microscopic diagrammatic theory. Both theories do not account for interaction. The first possibility is the dominant role of interaction. As seen in Fig. 2 and 3, going from 38 mK to 300 mK, the mean conductance changes by an amount $\delta\langle g \rangle_{ee}$, larger than the conductance fluctuations. One would expect that interaction corrections to the UCF part $\langle gg \rangle$ and higher order cumulants can be large enough to distort the gaussian. As the one-parameter scaling results in the gaussian distribution, assuming the Einstein relation between the conductance and the diffusion coefficient $\sigma = e^2 N(0) D$, the effect of interaction on the fluctuations of density of states $N(0)$ may be important.

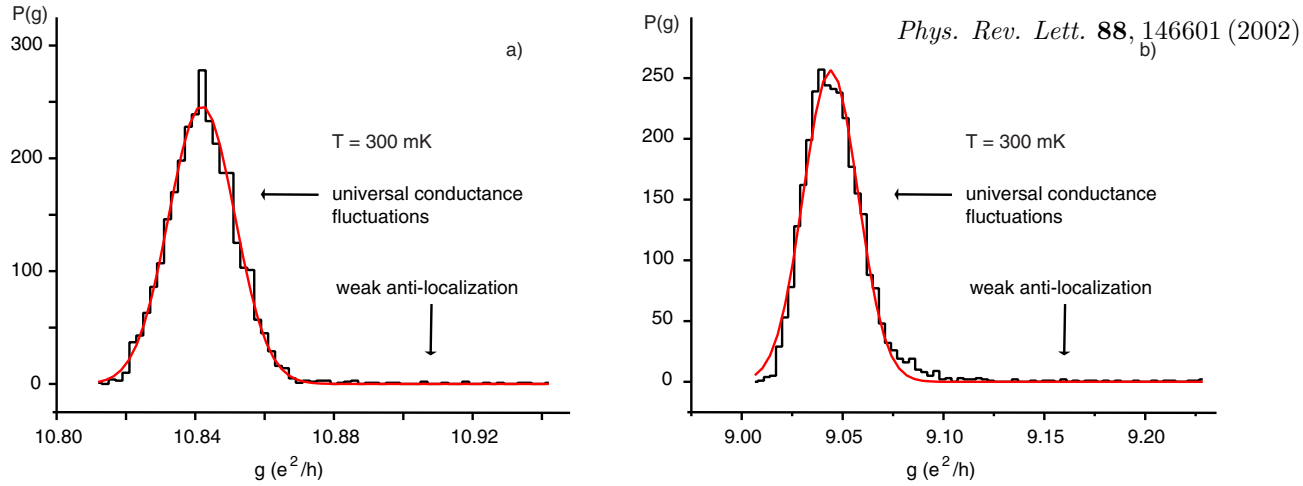

FIG. 3. Conductance of the same two quasi-1D Au wires (displayed in Fig. 2) at 300 mK with respective mean conductances of (a) 10.84 and (b) 9.05; the shift in the mean is due to the electron-electron interaction.

Another possibility is that the perturbative treatment of conductance in terms of $1/g$ as the expansion parameter is inadequate, even though g is large enough ($g \sim 8-10$) for the perturbative expansion to hold. The non-zero value of $\langle ggg \rangle$, contrary to the diagrammatic calculations, may require a new non-perturbative analysis.

In summary, we report the observation of non-gaussian conductance distribution in low-conductance metallic quasi-1D wires at low temperature (with greater than 3 sigma confidence level). This is not expected in random matrix theory or perturbative diagrammatic theory. The necessity of additional parameters, or cumulants, to describe the conductance possibly signals the breakdown of the one-parameter scaling hypothesis. This research is supported by NSF Gant No. DMR-9510416 and NSA Grant No. MDA90498C2194.

[1] E. Abrahams, P.W. Anderson, D.C. Licciardello, and T.V. Ramakrishnan, Phys. Rev. Lett. **42**, 673 (1979).
[2] L.P. Gorkov, A.I. Larkin, and D.E. Khmelnitskii, JETP Lett. **30**, 228 (1979).
[3] F. Wegner, Z. Phys. B **35**, 207 (1979); K.B. Efetov, Adv. Phys. **32**, 53 (1983).
[4] P.W. Anderson, D.J. Thouless, E. Abrahams, D.S. Fisher, Phys. Rev. B **22**, 3519 (1980).
[5] C.P. Umbach, S. Washburn, R.B. Laibowitz, and R.A. Webb, Phys. Rev. B **30**, 4048 (1984).
[6] P.A. Lee and A.D. Stone, Phys. Rev. Lett. **55**, 1622 (1985); B.L. Altshuler, JETP Lett. **41**, 648 (1985).
[7] B.L. Altshuler, V.E. Kravtsov, and I.V. Lerner, Sov. Phys. JETP **64**, 1352 (1986).
[8] A.D. Stone, K.A. Muttalib, and J.-L. Pichard, in *Anderson Localization*, edited by T. Ando, and H. Fukuyama (Springer-Verlag, 1988).
[9] K. Slevin, P. Markos, and T. Ohtsuki, Phys. Rev. Lett. **86**, 3594 (2001).
[10] K.A. Muttalib and P. Wolfle, Phys. Rev. Lett. **83**, 3013 (1999).
[11] A.M.S. Macedo, Phys. Rev. B **49**, 1858 (1994).
[12] "Quasi-one dimension" in the models based on the Landauer formalism implies that the cross-sectional dimensions are smaller than—or, comparable to—the mean free path for elastic scattering l_e and much larger than the fermi wavelength.
[13] M.C.W. van Rossum, I.V. Lerner, B.L. Altshuler, and Th. M. Nieuwenhuizen, Phys. Rev. B **55**, 4710 (1997); M.C.M. van Rossum, and Th. M. Nieuwenhuizen, Rev. Mod. Phys. **71**, 313 (1999); A.V. Tartakovski, Phys. Rev. B **52**, 2704 (1995).
[14] N. Kumar, J. Phys. C: Solid State Phys. **16**, L109 (1983); N. Kumar and A.M. Jayannavar, *ibid.* **19**, L85 (1986).
[15] For experiments in the Anderson localization regime see W. Poirier, D. Mailly, and M. Sanquer, Phys. Rev. B **59**, 10856 (1999); F. Ladieu, D. Mailly, and M. Sanquer, J. de Physique I **3**, 2321 (1993).
[16] A.D. Benoit, S. Washburn, C.P. Umbach, R.B. Laibowitz, and R.A. Webb, Phys. Rev. Lett. **57**, 1765 (1986).
[17] P.A, Lee, A.D. Stone, and H. Fukuyama, Phys. Rev. B **35**, 1039 (1987).
[18] A. Stuart and J.K. Ord, *Kendall's Advanced Theory of Statistics*, 5th edition (London, Griffin and Co. 1987).

Table 1. The mean $\langle g \rangle$ and the higher order moments of conductance for two high-g and two low-g metallic samples at 38 mK. The sampling errors in $\langle ggg \rangle$ and $\langle gggg \rangle$ with respect to a normal distribution are $\sqrt{6/N}$ and $\sqrt{96/N}$ respectively [18]. Note that $\langle ggg \rangle$ is not affected by Sheperd's correction for grouping [18].

Sample	L (μm)	w(nm)	t(nm)	R(Ω)	$\langle g \rangle$	$\langle gg \rangle$	$\langle ggg \rangle$	$\langle gggg \rangle$
1d-A	2.95	35.7	22	69	372.39	0.33	-0.015±0.035	-0.29±0.14
1d-B	2.95	26.7	22	56	473.39	0.65	-0.020±0.035	0.17±0.14
1d-C	20.3	30.0	18	2390	10.75	0.00055	0.164±0.025	-0.27±0.10
1d-D	20.3	30.0	18	2886	8.85	0.00171	0.087±0.025	-0.06±0.10